**Wolf-Rayet Stars**
*W.-R. Hamann, A. Sander, H. Todt, eds.*
*Potsdam: Univ.-Verlag, 2015*
*URL: http://nbn-resolving.de/urn:nbn:de:kobv:517-opus4-84268*

# Evolution of Wolf-Rayet spectra

**A. Liermann**[1]
[1] *Leibniz-Institut für Astrophysik Potsdam (AIP), Germany*

Wolf-Rayet stars are important sources for the enrichment of the ISM with nuclear processed elements, UV photons and momentum. They are descendants of high-mass stars for which short lifetimes and transition times can hamper the spectral classification of the stars in their different evolutionary phases. The expanded stellar atmospheres of Wolf-Rayet stars can show spectra which seem inconsistent with the anticipated underlying evolution phase, for example in late hydrogen-burning WN stars and Of/WN transition stars. We present a sequence of synthetic spectra of the Potsdam Wolf-Rayet models based on the latest Geneva stellar evolution models. This will visualize the changes in stellar spectra over a full stellar lifetime. Direct comparison with observed stellar spectra, as well as the evolution of diagnostic line ratios will improve the connection of spectral classification and evolution phase.

## 1 Motivation

The spectral classification of high-mass stars can be hampered by many factors, for example, the observed wavelength range with limited numbers of characteristic lines, diluted lines due to a high flux contribution from a binary companion, a short lived stellar evolution phase with the lack of templates for comparison, and so on.

Also, radiative-driven stellar winds like in Wolf-Rayet (WR) stars mask direct observations of the photosphere. For proper spectral classification and to determine stellar and wind parameters we rely on observed characteristic (wind) lines and the comparison to adequate models of expanding stellar atmospheres. The evaluation of observations and derived stellar parameters in the context of stellar evolution is still a challenge, for example to estimate the age and initial mass range of a star by comparison with stellar evolution tracks.

Stellar evolution models provide such tracks with well defined observable stellar parameters like temperature, magnitude, and surface abundance in connection with the underlying physical processes like rotational mixing or central burning processes. Groh et al. (2014) used the Geneva evolution tracks to compute CMFGEN models for a 60 $M_\odot$ star (Hillier & Miller 1998) and analyze the synthetic spectra in terms of spectral subtype assignment and stellar evolution.

In this work, we explore the use of stellar evolution models to create normalized synthetic spectra and flux-calibrated spectral energy distributions (SEDs) with model atmospheres further to support the spectral classification and thus understanding of various stellar evolution phases. We construct a grid of Potsdam Wolf-Rayet (PoWR) model atmospheres (e.g., Gräfener et al. 2002; Hamann & Gräfener 2004) for stellar evolution tracks of different initial stellar masses. This will enable us to study in detail the line profile variation, spectral transition phases, and evolution of quantities such as wind momentum, ionizing flux, etc. In addition, the available synthetic spectra can serve as templates for spectral classification throughout the high-mass regime in the Hertzsprung-Russell diagram.

## 2 Model grid

### 2.1 Potsdam Wolf-Rayet model atmospheres

We used the PoWR models to calculate normalized synthetic (emission) line spectra and spectral energy distributions.

The models assume spherically symmetric, stationary mass-loss with a prescribed velocity field; a $\beta$-law is adopted for the supersonic part of the stellar atmosphere, with the terminal velocity $v_\infty$ as a free parameter and $\beta = 1$ in this work. The velocity field in the subsonic region is defined so that a hydrostatic density stratification is approached.

The inner boundary of the model atmosphere, the "stellar radius" $R_*$, corresponds to a Rosseland optical depth of 20. And the "stellar temperature" $T_*$ is linked to the luminosity $L$ and the stellar radius $R_*$ via the Stefan-Boltzmann law.

The PoWR models account for wind inhomogeneities ("clumping") in a first-order approximation, assuming that optically thin clumps fill a volume fraction $f_\mathrm{V}$ and the inter-clump space is void. We specify a clumping factor $D = f_\mathrm{V}^{-1} = 4$ in this work. The Doppler velocity $v_\mathrm{dop}$, which reflects random motions on small scales ("microturbulence"), is approximated as one tenth of the terminal velocity and thus might vary from model to model along the evolution track (see below).

### 2.2 Model input

Calculated PoWR models are based on the stellar evolution tracks provided by the Geneva group (Ekström et al. 2012) for solar metallicities, with and without the effects of rotation. As model input, the evolution tracks provide per time step the parameters temperature, luminosity, mass-loss rate and

chemical surface abundances as listed in Table 1. For stars on the main sequence up to turn-off we used the effective temperature $T_{\rm eff}$ rather then the one not corrected for thickness of the stellar wind $T_*$.

**Tab. 1:** PoWR model input parameters from (1) Ekström et al. (2012), (2) Kudritzki & Puls (2000), (3) Hamann et al. (2006), (4) Sander et al. (2012).

| Parameter | | Reference |
|---|---|---|
| $T_{\rm eff}$, $T_*$, $\log(L/L_\odot)$ | | (1) |
| $\dot{M}$, $X$, $Y$, $X_{\rm CNO,surf}$ | | (1) |
| $v_\infty \cong$ | | |
| $f \cdot v_{\rm esc}$ | O stars | (2) |
| 1000 km/s | WN with hydrogen | (3) |
| 1600 km/s | WN without hydrogen | (3) |
| 2000 km/s | WC/WO | (4) |

The terminal velocity $v_\infty$ during the main-sequence up to turn-off time is derived via the escape velocity following Kudritzki & Puls (2000) with a factor $f$ depending on the effective temperature of the star. For the later evolution phases we list the fixed values and references in Table 1.

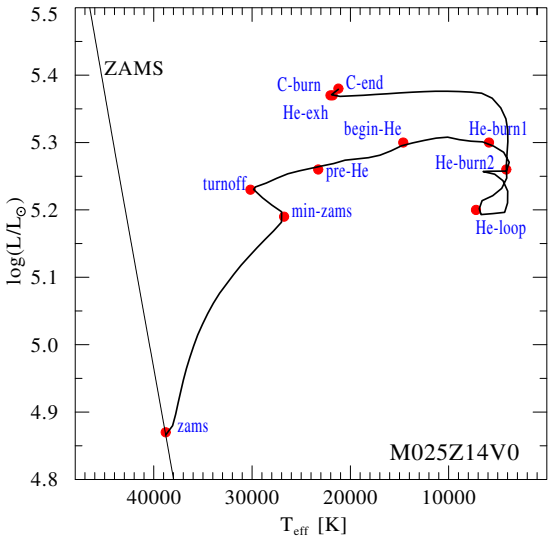


**Fig. 1:** Sampling of time steps for calculating PoWR models along the evolution model for a star with 25 $M_\odot$ initial mass without effects of rotation.

## 2.3 Sampling the evolution track

The Geneva evolution tracks comprise 400 time steps for a given initial mass. Computation-wise, it is infeasible to compute 400 PoWR models for each evolution track. Thus, input parameters are taken from selected time steps sampling the most significant phases in stellar evolution. This sampling follows the normalization scheme given by Ekström et al. (2012) and covers the main sequence towards turn-off, helium burning phases including a loop in the HR diagram, and carbon burning phases as shown in Fig. 1. Sub-grid sampling to cover transition phases in stellar evolution such as turn-off to possible luminous blue variable (LBV) phase can be calculated in a future project.

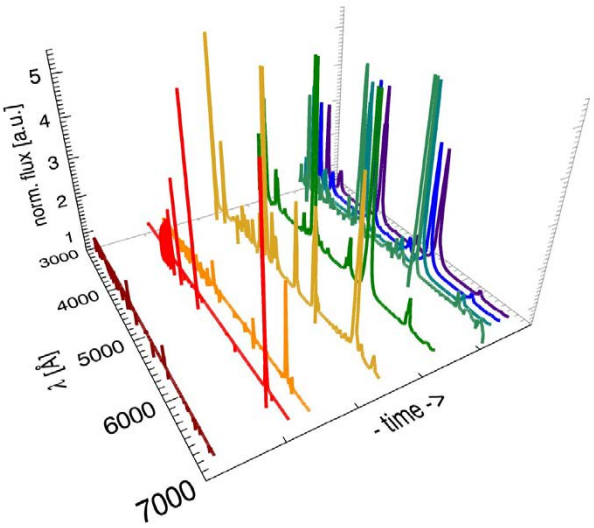


**Fig. 2:** Time sequence of PoWR spectra for an initial 60 $M_\odot$ star without effects of rotation.

# 3 Results

The grid of calculated PoWR models covers the evolution tracks of 25, 40, and 60 $M_\odot$ initial mass so far, each with $v_{\rm rot} = 0.4\, v_{\rm crit}$ and without the effects of rotation. Extension of this grid to other initial masses is considered for future work. In the following we focus on the track for 60 $M_\odot$ without rotation.

The output of the PoWR models summarizes the stellar parameters, including the input parameters, absolute magnitudes in different filter systems, and emergent astrophysical flux at each time step. More importantly the PoWR models provide synthetic (emission) line spectra and spectral energy distributions. The wavelength range of those covers the UV and Optical (1200–7800 Å), Helium I (9500–12000 Å) in detail, and near-infrared JHK (1–2.5 $\mu$m) regime for this work. The sequence of optical spectra across time following the evolution track is shown in Fig. 2.

Depending on the specific interest, the available grid allows for different aspects to be analyzed both individually per time step and in total in the framework of stellar evolution:

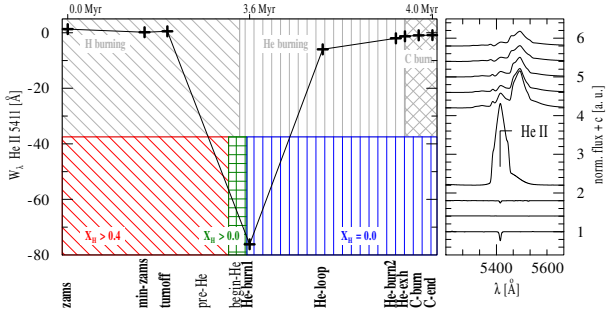


**Fig. 3:** Evolution of $W_\lambda$ of a He II line. The background (left panel) represent the ongoing central burning process and hydrogen surface abundances of the according evolution track. Normalized emission line spectrum (right panel) flux plus constant shift over time.

(i) direct comparison to observed spectra for line identification and spectral classification,

(ii) correlation of properties of diagnostic lines in different wavelength regimes,

(iii) SED fitting to obtain reddening and distance/luminosity estimates,

(iv) spectral line profile fitting to derive stellar and wind parameters,

(v) evolution of line properties, like equivalent width, FWHM, and line ratios, and

(vi) energy and momentum output over stellar lifetime.

As an example, we present the evolution of the equivalent width $W_\lambda$ of the He II line at $\lambda 5411$ Å in Fig. 3. It can be clearly seen that during main-sequence evolution, associated with the hydrogen burning phase, the line is hardly present in the spectrum but becomes a prominent emission line for the Wolf-Rayet phases. The pattern and color coding of the background helps to distinguish between hydrogen-depleted or hydrogen-free atmospheres for these later phases. Also the underlying central burning process of the evolution model might help to classify transition phases, for example, between O stars leaving the main sequence and very late WN stars.

In Fig. 4, we present the evolution of absolute Johnson magnitudes over time (top panel) as well as the number of ionizing photons for hydrogen and helium (bottom panel). The biggest changes in the number of ionizing photons are found towards the end of the main-sequence life with a decrease of the order of a magnitude. Over the remaining stellar lifetime the numbers remain at an about constant level.

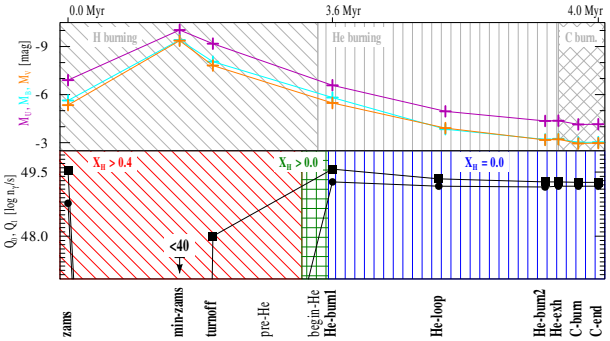


**Fig. 4:** Evolution of absolute magnitudes (top panel) and ionizing photons for H ($Q_0$, crosses) and He I ($Q_1$, circles), respectively (bottom panel). See Fig. 3 for explanation of the background pattern.

In the ongoing analysis, we will relate spectral subtypes to the evolution phases. This will allow also a better understanding of findings like line-profile or emergent-flux changes in the context of stellar evolution to be established.

The grid of models will be available upon request.

## Acknowledgments

I am thankful to the present PoWR team (Wolf-Rainer Hamann, Helge Todt, Andreas Sander, Rainer Hainich, Tomer Shenar) for providing and maintaining the model atmosphere code and helpful discussion during this project.

## References

Ekström, S., Georgy, C., Eggenberger, P., et al. 2012, A&A, 537, A146

Gräfener, G., Koesterke, L., & Hamann, W.-R. 2002, A&A, 387, 244

Groh, J. H., Meynet, G., Ekström, S., & Georgy, C. 2014, A&A, 564, A30

Hamann, W.-R. & Gräfener, G. 2004, A&A, 427, 697

Hamann, W.-R., Gräfener, G., & Liermann, A. 2006, A&A, 457, 1015

Hillier, D. J. & Miller, D. L. 1998, ApJ, 496, 407

Kudritzki, R.-P. & Puls, J. 2000, ARA&A, 38, 613

Sander, A., Hamann, W.-R., & Todt, H. 2012, A&A, 540, A144

**Anthony (Tony) Moffat:** Can you convert your predicted spectral variations into variations in spectral subtype? This would be very useful for observers. Do you see evidence for the peeling-off scenario?

**Adriane Liermann:** This is work in progress, and we plan to do the spectral classification and assign subtypes for the evolution phases. On the second part of your comment I'd like to pass on to José for an answer.

**José Groh:** We do see an evolution of spectral types during the WN phase as the hydrogen envelope is peeled off. However, during the WC phase we see a quite constant spectral type.